TRENDS IN SCIENCES 2026; 23(6): 12373
https://doi.org/10.48048/tis.2026.12373 RESEARCH ARTICLE

Fabrication and Cytotoxicity Testing of Silver Nitrate Modified PETG Scaffolds for Bone Applications

Hussein Mishbak[1,*], Evangelos Daskalakis[2,3], and Mohamed Hassan[2]

[1]*Department of Biomedical Engineering, Collage of Engineering, The University of Thi-Qar, Thi-Qar, Iraq*
[2]*Department of Mechanical, Aerospace, and Civil Engineering, University of Manchester, Manchester, United Kingdom*
[3]*Singapore Centre for 3D Printing, School of Mechanical and Aerospace Engineering, Nanyang Technological University, Singapore*

([*]Corresponding author's email: Hussein.mishbak@utq.edu.iq)

Received: 21 October 2025, Revised: 1 November 2025, Accepted: 8 November 2025, Published: 30 January 2026

Abstract

This study examines the surface modification of 3D printed polyethylene terephthalate glycol (PETG) scaffolds by a simple and reproducible coating method using silver nitrate ($AgNO_3$) and the cytotoxicity of the modified scaffolds is assessed. The main aims of the study were characterization of the structural and morphological changes on the surface of the scaffold after the treatment, more precisely the thickness of the deposited silver coating, and assessment of the biological effect on the HBL100 normal cell lines. The chemical protocol for scaffold modification was a multi-step process including the preparation of silver nitrate solution, a necessary pre-treatment of PETG scaffold using a sodium hydroxide (NaOH) solution, immersion of scaffold in the $AgNO_3$ solution, sonication and final drying process. Atomic Force Microscopy (AFM) analysis was performed to measure the thickness of the coating, finding a high dependence of the coating on the 3D printing angle of the scaffold. The PETG scaffold with 0°/45° had a coating thickness of about 566 nm, which was much thicker than coatings on scaffolds with 0°/60°/120° and 0°/90° printing laydown patterns. The cytotoxicity of the scaffolds was tested by the standard MTT assay. The results of the assay including mean absorbance, mean inhibition percentage and standard deviation showed no significant cytotoxic effect from the coated scaffolds with the mean inhibition percentages ranging from a minimal 0.74% to 10.91%. This study demonstrates a viable and biocompatible method to functionalize 3D-printed PETG scaffolds which could have significant implications for various applications including tissue engineering and medical devices where the need to both structural integrity and non-toxic surface properties is paramount.

Keywords: PETG, silver nitrate ($AgNO_3$), Coating, 3D printing, Surface modification, Laydown patterns, Bone tissue applications, Cytocompatibility

Introduction

Three-dimensional printed scaffolds made of polyethylene terephthalate glycol (PETG) have been considered as promising candidates for bone tissue engineering application because of their superior mechanical properties compared to conventional polymers like polycaprolactone (PCL) with excellent biocompatibility and printability [1,2]. PETG scaffolds have compressive moduli and strengths that are similar to human trabecular bone, and thus are mechanically appropriate for load-bearing bone regeneration [3,4]. However, one of the major drawbacks in bone tissue engineering is the prevention and management of bacterial infections at the implant site that can result in osteomyelitis and implant failure [5,6]. To tackle this issue, the integration of antimicrobial agents into scaffold systems has become an indispensable approach to fabricating multifunctional biomaterials for

supporting bone regeneration and at the same time to prevent bacterial colonization [7-9].

In particular, silver-based antimicrobial systems, especially silver nitrate ($AgNO_3$), have received much attention because of their wide-spectrum antimicrobial activity against both Gram-positive and Gram-negative bacteria including multidrug-resistant strains [10,11]. $AgNO_3$ coating on polymer scaffold releases silver ions (Ag^+) which exhibit bactericidal effects through various mechanisms such as damage to bacterial cell membrane, inhibition of respiratory enzymes, condensation of DNA and production of reactive oxygen species inside bacterial cells [12,13]. The coating of PETG scaffolds with $AgNO_3$ is a new characterization technique, which converts these biocompatible structural scaffolds into bioactive platforms for controlled delivery of antimicrobial agents [14,15]. The silver ion release from the scaffold over long periods of time allows for a surface modification strategy that would supply therapeutic levels of silver ions for prolonged periods that would be beneficial during the critical early phases of bone healing to provide antimicrobial protection [11,16].

However, the use of silver-based antimicrobial coatings into bone tissue engineering scaffolds represents a delicate balance between the performance of bactericidal activity and cellular biocompatibility [17,18]. The cytotoxicity of silver ions is a concentration-dependent process that plays an important role on the biological behavior of $AgNO_3$ coated scaffolds [19,20]. Although silver ions are effective against pathogenic bacteria, high concentrations can have a negative impact on osteogenic cells, which can negatively impact the osteoblast proliferation and differentiation and mineralization processes that are critical for successful bone regeneration [20]. Studies have shown that Ag^+ concentrations of 1.0 - 1.5 ppm can disrupt osteogenic differentiation by altering the gene expression profile including the downregulation of collagen type I (COL1A2) and alkaline phosphatase (ALP) and thus matrix mineralization [21]. On the other hand, optimized lower concentrations ($\leq$ 0.5 ppm) have been proved to be sufficient to allow undisturbed osteogenic differentiation while retaining the antimicrobial efficacy [22].

Interestingly, recent studies have shown that silver nanoparticles, which are different from the ionic silver, can paradoxically induce osteogenic differentiation of mesenchymal stem cells through activation of RhoA signaling pathway resulting in actin polymerization and increased cytoskeletal tension [18]. This osteoinductive effect has been noted at concentrations that keep low cytotoxicity, with silver nanoparticles showing the ability to upregulate important osteogenic markers such as Runt-related transcription factor 2 (RUNX2), osteopontin (OPN) and collagen type I (COL1A1) [23]. Furthermore, the silver delivery mode (nanoparticles or $AgNO_3$ coating with ionic release) has a significant impact on the antimicrobial effect and cellular response, and controlled release kinetics is of great importance to achieve therapeutic effects [24].

The characterization of $AgNO_3$-coated PETG scaffolds for bone applications therefore needs to include a thorough evaluation of a number of parameters such as surface morphology, silver release kinetics, antimicrobial activity against clinically relevant pathogens and *in vitro* biocompatibility with osteogenic cells [25].

Surface modification is an outstanding technique in overcoming the limitations of PETG and other polymers, by introducing new qualities in the material without modifying the bulk properties [26-28]. The approach of coating a silver layer onto a polymer scaffold provides a functionalized surface that is able to resist bacterial colonization, an important property for implants and scaffolds in a biological environment [29,30]. However, the dose-dependent nature of silver effects (therapeutic agent at low concentration and cytotoxic agent at high concentration) requires careful examination of the biocompatibility of any new silver-modified material [20,31]. Silver nanoparticle-polymer nanocomposites are a transformative development, with the polymer matrix itself serving as a stabilizing medium, reducing nanoparticle aggregation and helping to overcome the cytotoxicity associated with free silver nanoparticles while maintaining robust antimicrobial activity [32,33].

The combination of mechanical stability of PETG and the antimicrobial activity of $AgNO_3$ is a premeditated approach towards the construction of next-generation bone scaffolds that can simultaneously fulfill the structural, biological, and antimicrobial demands for effective treatment of bone defects especially in infection-prone clinical settings [34,35].

This study was perceived to fill the gap between the structural utility of the 3D printed PETG scaffolds and the need for increased functionality in bone regeneration applications. The main goal was to establish and characterize a simple chemical method for coating 3D printed PETG scaffolds with silver nitrate ($AgNO_3$) to produce a functionalized surface. This was succeeded by the extension of the experiment to 2 important areas of the deposited silver layer; physical characterization of the deposited layer with respect to thickness and scaffold geometry; and a more detailed cytotoxicity experiment, to establish the biocompatibility of the treated material with normal cell lines. A major advantage of this research is that it has been shown that the 3D printing laydown pattern can be used to directly control the thickness and morphology of the resulting silver coating. While surface modification of polymers is well documented, and Khan *et al.* [36] was able to coat the scaffolds with silver by repeated immersion cycles (50 times) to produce antimicrobial scaffolds. This approach is unique in that surface engineering is integrated into the initial scaffold design phase by varying the printing angle alone (0°/45°, 0°/60°/120° and 0°/90°) we were able to obtain controllable coating thicknesses. This allows a more efficient and predictable way of tuning surface properties from the beginning in comparison to multi-step coating procedures.

Materials and methods

Materials

The main chemicals and reagents used for coating the scaffolds and cytotoxicity testing were purchased from different international suppliers to ensure their quality and reproducibility. Sodium hydroxide (NaOH) was purchased from (Lobachemie, India) and silver nitrate ($AgNO_3$) was purchased from (Daejung, Korea). Trypsin/EDTA, needed to dissociate cells, was obtained from (Capricorn, USA). As an organic solvent for different procedures, dimethylformamide (DMF) was purchased from (Santa Cruz, USA).

Essential media and biological reagents were included in RPMI 1640 and fetal bovine serum which were supplied by (Gibco, USA). For the cytotoxicity tests the MTT stain was used, which was obtained from (Sigma, USA). Cell culture plastics, including cell culture plates and microtiter readers were supplied by (Thermo Fisher Scientific, USA). Instruments required to perform the experimental procedures, including the CO_2 incubator and micropipette, were provided by (Cypress Diagnostics, Belgium). For the purpose of maintenance of sterile condition, laminar flow hood was utilized, which was purchased from (K & K Scientific Supplier, Korea). All the reagents, chemicals and instruments were therefore carefully chosen from reputed manufacturers in India, Korea, USA and Belgium, and standardized and reliable experimental conditions were ensured.

Methods

Scaffold preparation and coating procedure

PETG scaffolds were fabricated following the procedure published in our previous study [37]. The PETG scaffolds were initially rinsed with deionized (DI) water to remove dust or debris left over from the fabrication process. A pre-treatment step was then carried out by soaking the scaffolds in 2% NaOH solution for 5 min to activate the surface of the PETG, which is an essential step for a better adhesion of the subsequent $AgNO_3$ coating [38,39]. The alkaline treatment, that is a topochemical reaction mainly affecting the fiber surface, causes hydrolysis of polymer chains leading to an increase in the number of terminal hydroxyl and carboxyl groups and altered the wettability of the surface [39]. After NaOH pre-treatment, scaffolds were again rinsed with DI water and patted dry.

Prepare the silver nitrate solution

$AgNO_3$ solution was prepared by dissolving 10 g of $AgNO_3$ powder in 100 mL of DI water. $AgNO_3$ solution was divided into 4 parts of 25 mL (1 mg/mL). The solution was slowly stirred on a hotplate magnetic stirrer until the All of $AgNO_3$ was dissolved. In order to avoid the precipitation of silver oxide, which may take place in the presence of an alkaline medium, sodium hydroxide tablets were added step by step to the solution until pH 9 was reached.

In order to protect the photosensitive solution from a light-induced reduction, the beaker was covered with aluminum foil. Scaffolds were soaked for 20 - 30 min, while being gently stirred to facilitate even coating. The scaffolds were then immersed into ultrasonic bath for 2 h at low temperature in order to ensure that all parts of

the scaffold were uniformly coated with $AgNO_3$. Ultrasound irradiation is an effective method for coating nanoparticles because the micro-bubbles that are generated by cavitation can generate microjets and shockwaves that can aid in the physical deposition of nanoparticles onto the substrate. Finally, the coated PETG scaffolds were dried in an oven at 45°C. All steps are clarified by **Figure 1**.

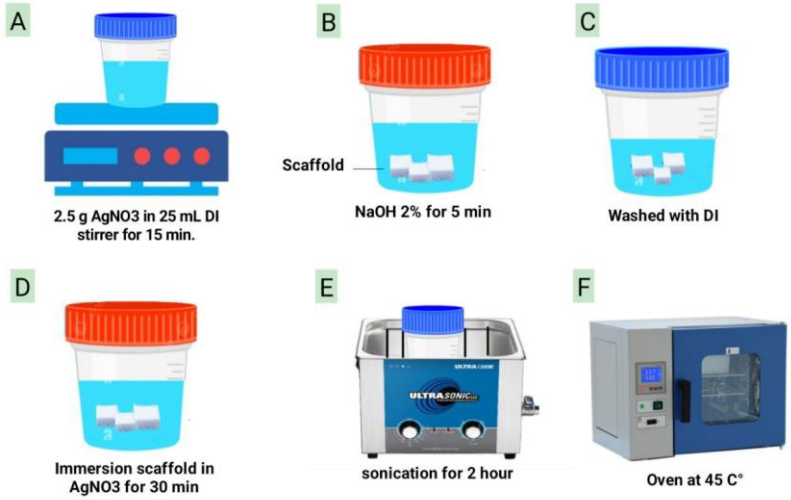

Figure 1 Schematic illustration of silver-nitrate coating scaffold prepared in 6 steps. (A) 0.1 M solution of silver nitrate ($AgNO_3$) 25 mL. is made by dissolving 2.5 g $AgNO_3$ in DI (deionized) water and mixing after 15 min. (B) Pre-treatment of a scaffold with 5 min of immersion in 2% sodium hydroxide (NaOH) solution ensues. (C) DI water is used to wash the scaffold to remove remnants of NaOH. (D) Then the scaffold is dipped in the $AgNO_3$ prepared solution for 30 min. (E) A 2-hour sonication action is then performed on the scaffold. (F) The scaffold is dried in the oven at 0 ℃/45 °C.

Characterization

Biological assessment

The HBL100 normal cell lines which were cultured in RPMI-1640 with 10% Fetal bovine, 100 units/mL penicillin and 100 µg/mL streptomycin. Cells were reseeded twice or thrice every 70% confluence with Trypsin-EDTA and cultured at 37 °C and 5% CO_2 [40].

Atomic force microscopy characterization

The coated and uncoated PETG scaffolds were examined visually, since the color difference was used as a preliminary measure of the surface coating. Atomic force Microscopy (AFM) was then used to quantitatively determine the thickness of the silver coating. AFM is a highly popular and suitable method of studying topography and roughness of the surfaces on a nanoscale. The examined scaffolds were printed at various angles of 0°/45°, 0°/60°/120° and 0°/90°. AFM analysis was conducted to determine the association between scaffold's geometry and coating properties. The AFM scan images were also used to analyze the morphology of the surface post coating process.

Cytotoxicity assays (MTT)

Determination of the cytotoxic effect of the coated scaffolds was preformed based on the MTT cell viability assay in 96-well plates. HBL100 normal cell lines were obtained in the IRAQ Biotech Cell Bank Unit in Basrah and were cultured in RPMI-1640 containing 10% Fetal bovine serum, 100 units/mL penicillin, and 100 ug/mL streptomycin. HBL100 normal cell lines were passaged 3-fold to 2 times a week at 70% confluency using Trypsin-EDTA.

In the assay, cells were seeded at a concentration of 1×10^4 cell/well. After 24 h or when a confluent monolayer was obtained, 6 types (0°/45°, 0°/60°/120° and 0°/90° coated and uncoated) of scaffolds were inserted in the wells in 4 replicates each. After 72 h of treatment cell viability was assessed. The medium and scaffolds were removed and 28 µL of a 2 mg/mL solution of MTT were added. The cells were incubated

and after the removal of MTT solution, the formazan crystals that were left in the wells were solubilized by adding 100 µL of DMSO (Dimethyl Sulphoxide). Incubation under shaking at 37 °C was then completed. The microplate reader at 620 nm was used to determine the absorbency. This was performed in triplicate.

The rate of cell growth inhibition (percent of cytotoxicity) was determined by use of the following equations:

$$PR = AB \times 100 \quad (1)$$

PR: is the proliferation rate, A: is the average optical density of the untreated wells (negative control), and B: is the optical density of the treated wells. Then the rate of inhibition (IR) was determined as:

$$IR = 100 - PR \quad (2)$$

Statistical analysis

The analysis of variance (ANOVA) was applied to question the data one-way, and post-hoc analysis was conducted using Tukey. Differences were considered statistically significant at * $p < 0.05$, ** $p < 0.01$, *** $p < 0.001$ and **** $p < 0.0001$. GraphPad Prism software (GraphPad Software Inc., San Diego, CA, USA) was used in this research.

Results and discussion

Scaffold visualization

The color of the coated and uncoated scaffolds was observed visually to have changed successfully, which means that a new layer was deposited on the scaffolds. The texture of the surface of the coated scaffolds was more particulate in nature than the smooth surface of the uncoated PETG scaffolds. Four 3D-printed PETG scaffolds are shown in this **Figure 2**, from left to right, 0°/90°, 0°/60°/120°, 0°/45° laydown pattern and the scaffold in the far right is the control sample. The color contrast between the samples shows the difference in coating thickness on the surface of the PETG and was measured by atomic force microscopy (AFM). The control sample is uncoated which is indicated by the lighter color.

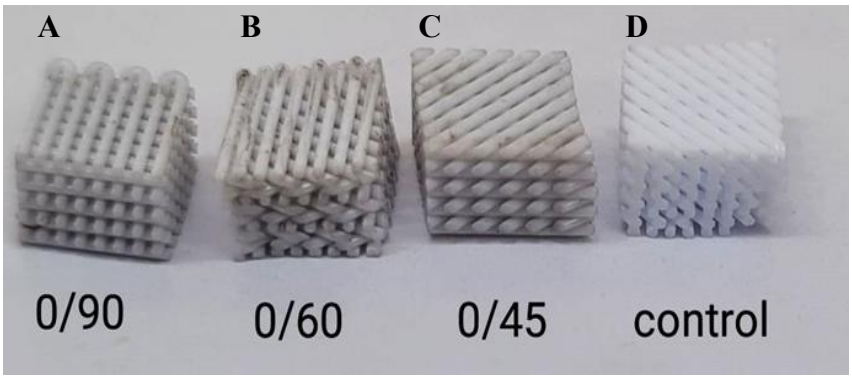

Figure 2 The PETG scaffold coated/uncoated: (A) coated 0°/90°, (B) coated 0°/60°/120°, (C) coated 0°/45°, (D) control.

Scaffold characterization

Atomic Force Microscopy (AFM) was used as the main characterization method to quantify coating thickness, surface morphology and coating uniformity for all types of scaffolds [41]. AFM is a nanometer resolution technique, which is extremely suitable for the measurement of thin film coatings on polymer scaffolds, and has a high sensitivity compared to conventional profilometry methods [41,42].

Type 1 Scaffolds (0°/45°) had the thickest silver coating with an average differential thickness of 566.7 nm. AFM height topography maps showed clear topographical features with the coated area (Plane 2) having a mean height of 623.8 nm as opposed to the uncoated substrate (Plane 1) at 57.07 nm. The maximum height of the coated area was 805.2 nm, which showed the presence of considerable vertical protrusions and high surface roughness. The relatively large angle difference of 12.15° between the 2 planes indicates an

uneven coating distribution with silver particle aggregation, which is probably caused by the higher porosity and internal surface area of the 0°/45° structure. Three-dimensional AFM reconstructions verified a very rough surface where micro-roughness could be observed as well as independent clusters of particles typical of silver nanoparticle aggregation could be observed. As depicted in **Figure 3**.

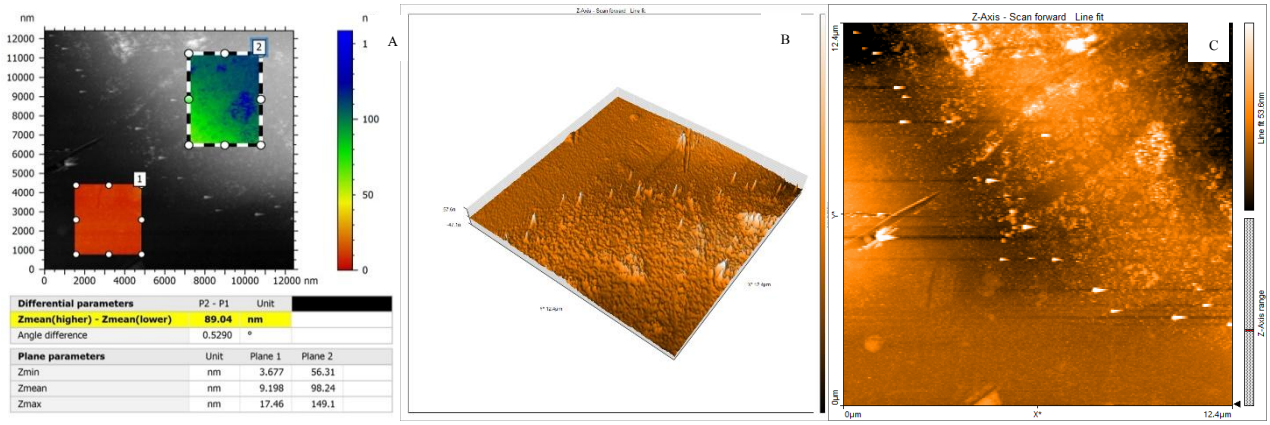

Figure 3 0°/45° coated scaffold (A) 2D AFM height map (inset: Phase image), (B) 3D AFM topography and, (C) SEM of silver-coated PETG.

Type 2 Scaffolds (0°/60°/120°) had a much thinner coating with a mean thickness of 89.04 nm. The coated surface (Zmean = 98.24 nm) was more homogeneous than Type 1 with a maximum height of 149.1 nm and a small angle difference (0.5290°), which showed good coating conformality and adhesion. The 2D AFM images revealed a smooth and continuous film with a finer grain structure and less surface heterogeneities. This intermediate coating thickness is an optimum between antimicrobial functionality and mechanical stability because thinner coatings are less likely to delaminate and crack under mechanical stress in **Figure 4** [44,45].

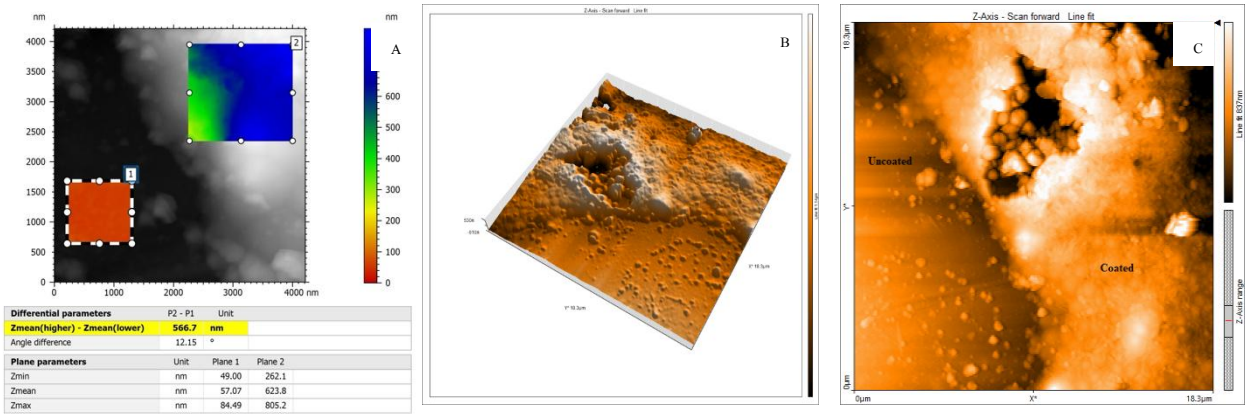

Figure 4 0°/60°/120° coated scaffold (A) 2D AFM height map (inset: phase image), (B) 3D AFM topography and, (C) SEM of silver-coated PETG.

Type 3 Scaffolds (0°/90°) revealed a coating thickness of 107.1 nm with the coated area having a mean height of 334.3 nm (Plane 2) and 227.2 nm (Plane 1). The angle difference was small (0.2493°), which indicated excellent coating uniformity over the surface. The higher Zmean baseline values for both planes indicate that the denser scaffold structure has a higher starting surface and thus, leads to a more homogeneous

coating distribution. The AFM phase image and 3D topography map of the scaffold showed a silver layer with uniformly distributed nanoscale features and less particle aggregation than the Type 1 scaffolds [46,47] in **Figure 5**.

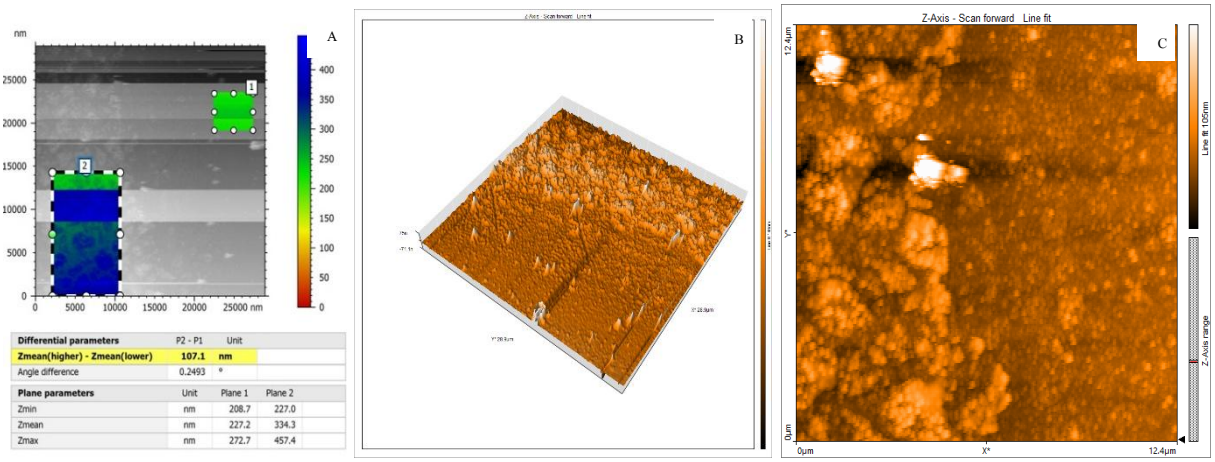

Figure 5 0°/90° coated scaffold (A) 2D AFM height map (inset: phase image), (B) 3D AFM topography and (C) SEM of silver-coated PETG.

The thickness of the silver nitrate layer is the difference between the coated and uncoated parts, that is, the difference of Z (Zmean (higher) − Zmean (lower)) = 566.7 nm for the 0°/45° scaffold and it is also applicable for other scaffolds. These quantitative data are important for validation of the coating process, and also ensure that the scaffold has surface properties that are required for the application for which it is intended. The AFM analysis revealed a rough and irregular surface of the 3D printed PETG scaffold coated with $AgNO_3$, consisting of nanoparticle aggregates resembling peaks and valleys. This nanoscale topography provides a high surface area and sites favorable for the adsorption of protein and cell seeding attachment.

While these surface irregularities can improve initial cell attachment, the rough surfaces can impede spreading in a uniform fashion. Furthermore, the coating thickness cannot be determined from AFM imaging alone and a step-height measurement is necessary to ensure layer stability and controlled silver ion release.

Cytotoxicity evaluation

The results of the MTT assay demonstrated that the silver-coated PETG scaffolds showed no significant cytotoxic effect on the HBL100 normal cell line under the experimental conditions. The mean inhibition percentages for the 6 different coated and uncoated scaffolds were consistently very low, ranging from a minimum of 0.74 ± 6.136 to a maximum of 10.91 ± 7.315 as shown in **Table 1**.

Table 1 MTT Assay results for coated and uncoated scaffolds.

Scaffold		Mean absorbance	Mean inhibition (%)	Sample size (n)
Uncoated	0°/45°	0.4555	0.74 ± 6.136	4
	0°/60°/120°	0.4548	0.89 ± 2.280	4
	0°/90°	0.4365	4.88 ± 4.287	4
Coated	0°/45°	0.4492	2.11 ± 3.770	4
	0°/60°/120°	0.4117	10.27 ± 6.570	4
	0°/90°	0.4088	10.91 ± 7.315	4

The low mean inhibition percentages are a direct and quantitative indicator that the silver coating method does not significantly harm the normal cells. This finding is reinforced by the relatively low standard deviations associated with the data, which indicate a consistent and uniform cellular response across the replicates, thereby increasing the reliability of the results. As shown in **Figure 6**.

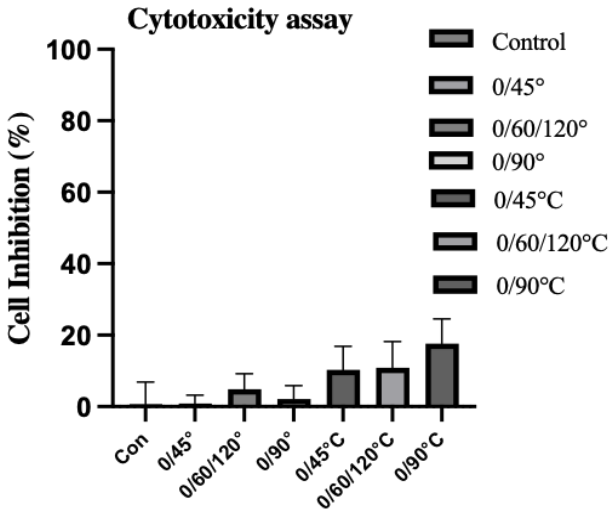

Figure 6 The inhibitory effect of 6 different scaffolds on the HBL100 cell line.

Discussion

The silver nitrate coating of the 3D printed PETG scaffolds resulted in clear coating thickness and morphology depending on the printing laydown pattern. The thickest coating (≈ 566 nm) was obtained in the 0°/45° configuration scaffold with considerable nanoparticle aggregation and high surface roughness, which is probably attributed to its higher internal surface area and porosity, which allow silver deposition. In contrast, the coatings on the 0°/60°/120° and 0°/90° scaffolds were much thinner (approx. 89 nm and 107 nm, respectively), more homogeneous and conformal (less than 0.53° of inter-plane angle difference) and finer grained. These moderate thicknesses are beneficial in sustaining mechanical stability during loading, elimination of the risk of delamination and cracking and still offer antimicrobial activity.

The nanotopographical features of the scaffolds observed by AFM indicate that the rough agglomerated surface of the 0°/45° scaffold could improve protein adsorption and primary cell attachment due to the increased binding sites. However, high roughness may hinder cell spreading uniformity and may cause local mechanical changes that play an important role for osteogenic differentiation. On the other hand, the smoother surfaces of the 0°/60°/120° and the 0°/90° scaffolds balance the surface area to uniformity ratio, and may provide more predictable interactions between cells and the materials, and controlled kinetics of silver ions release [48].

The cytotoxicity evaluation by the MTT assay showed low percentages of inhibition for all the coated scaffolds, which means that the silver nitrate coating process is biocompatible under the tested conditions. Further, the relatively low standard deviations are indicative of homogeneous cellular response. These results corroborate the fact that the silver concentrations released from the coatings are below cytotoxic levels for normal HBL100 cells, which is consistent with literature reports that optimized Ag^+ concentrations (≤ 0.5 ppm) will provide antimicrobial protection without affecting cell viability [49]. As a composite, all these findings indicate that the printing geometry can be deliberately used to adjust the silver coating thickness and the surface topography. By choosing suitable laydown patterns, it is possible to tune the antimicrobial efficacy, mechanical integrity and the cellular compatibility of PETG scaffolds for bone tissue engineering applications.

Conclusions

This study provided a simple and reproducible chemical method to coat 3D-printed PETG scaffolds with silver nitrate, most importantly, functionalization was achieved without affecting the cytocompatibility. The primary result was that the printing layup pattern (0°/45° vs. 0°/60°/120° and 0°/90°) has a tremendous effect on the resulting coating thickness and texture - from highly textured and thick to thinner and more uniform layers - allowing for precise control of the surface topography. The low cytotoxicity of all coated scaffolds indicates their high potential for bone regeneration applications, particularly when it is complicated by infection. The current research should now be aimed at measuring the dynamics of silver ion release, establishing the presence of antimicrobial activity on clinical pathogens, and *in vitro* osteogenic differentiation analysis to optimize the scaffold design to be used *in vivo*.

Acknowledgements

The authors express their sincere gratitude to the University of Thi-Qar, Iraq for their continuous support and facilitation in the completion of this research project. Special appreciation is also extended to Nanyang Technological University, Singapore, for providing valuable resources, technical guidance and collaborative opportunities that had made a significant contribution to the success of this study.

Declaration of Generative AI in Scientific Writing

The authors recognize the use of generative AI tools (e.g. QuillBot and Gemini by Google) to aid in the refinement of the language and grammatical editing during the preparation of this manuscript. AI tools were not used to create content, analyze or interpret data. Authors have full responsibility for the accuracy, integrity and conclusions of the work.

CRediT Author Statement

Hussein Mishbak and **Mohamed Hassan:** Conceptualization; Methodology; Software. **Hussein Mishbaj Evangelos Daskalakis:** Data curation; Writing - Original draft preparation. **Hussein Mishbak:** Visualization; Investigation. **Evangelos Daskalakis** and **Mohamed Hassan:** Software; Validation. **Hussein Mishbak** and **Evangelos Daskalakis:** Writing.

References

[1] J Meneses, JC Silva, SR Fernandes, A Datta, F Castelo Ferreira, C Moura, S Amado, N Alves and P Pascoal-Faria. A multimodal stimulation cell culture bioreactor for tissue engineering: A numerical modelling approach. *Polymers* 2020; **12(4)**, 940.

[2] G Iosub, IA Lungescu, AC Bîrcă, AG Niculescu, PC Balaure, S Constantinescu, B Mihaiescu, DM Rădulescu, AM Grumezescu, A Hudiță, IA Neacșu and AR Rădulescu. New three dimensional-printed polyethylene terephthalate glycol liners for hip joint endoprostheses: A bioactive platform for bone regeneration. *Materials* 2025; **18(6)**, 1206.

[3] MH Hassan, AM Omar, E Daskalakis, Y Hou, B Huang, I Strashnov, BD Grieve and P Bártolo. The potential of polyethylene terephthalate glycol as biomaterial for bone tissue engineering. *Polymers* 2020; **12(12)**, 3045.

[4] J Sun, H Zhu, H Wang, J Li, B Li, L Liu and H Yang. A multifunctional composite scaffold responds to microenvironment and guides osteogenesis for the repair of infected bone defects. *Journal of Nanobiotechnology* 2024; **22(1)**, 577.

[5] L Qin, S Yang, C Zhao, J Yang, F Li, Z Xu, Y Yang, H Zhou, K Li, C Xiong, W Huang, N Hu and X Hu. Prospects and challenges for the application of tissue engineering technologies in the treatment of bone infections. *Bone Research* 2024; **12(1)**, 28.

[6] JCC Paiva, L Oliveira, MF Vaz and S Costa-de-Oliveira. Biodegradable bone implants as a new hope to reduce device-associated infections - a systematic review. *Bioengineering* 2022; **9(8)**, 409.

[7] JCC Paiva, L Oliveira, MF Vaz and S Costa-de-Oliveira. Construction of antibacterial bone implants and their application in bone regeneration. *Materials Horizons* 2024; **11(3)**, 590-625.

[8] CT Johnson and AJ García. Scaffold-based anti-infection strategies in bone repair. *Annals of Biomedical Engineering* 2015; **43**, 515-528.

[9] M Li, P Zhao, J Wang, X Zhang and J Li. Functional antimicrobial peptide-loaded 3D

scaffolds for infected bone defect treatment with AI and multidimensional printing. *Materials Horizons* 2025; **12(1)**, 20-36.

[10] A Roy, P Basuthakur, S Haque and CR Patra. Silver-based nanoparticles for antibacterial activity: Recent development and mechanistic approaches. *In*: RN Krishnaraj and RK Sani (Eds.). Microbial interactions at nanobiotechnology interfaces: Molecular mechanisms and applications. Wiley, New Jersey, 2021, p. 245-301.

[11] M Mohiti-Asli, B Pourdeyhimi and EG Loboa. Novel, silver-ion-releasing nanofibrous scaffolds exhibit excellent antibacterial efficacy without the use of silver nanoparticles. *Acta Biomaterialia* 2014; **10(5)**, 2096-2104.

[12] SS Goderecci. 2016, Cytotoxic and antimicrobial effects of silver-containing surfaces. Master Thesis. Rowan University, New Jersey, 2016.

[13] L Xu, YY Wang, J Huang, CY Chen, ZX Wang and H Xie. Silver nanoparticles: Synthesis, medical applications and biosafety. *Theranostics* 2020; **10(20)**, 8996.

[14] E Hamidi. Antibacterial coating for aesthetic orthodontic devices, Available at: https://www.politesi.polimi.it/handle/10589/187701, accessed July 2025.

[15] D Flores, J Noboa, M Tarapues, K Vizuete, A Debut, L Bejarano, DA Streitwieser and S Ponce. Simple preparation of metal-impregnated FDM 3D-printed structures. *Micromachines* 2022; **13(10)**, 1675.

[16] X Wu, J Li, L Wang, D Huang, Y Zuo and Y Li. The release properties of silver ions from Ag-nHA/TiO2/PA66 antimicrobial composite scaffolds. *Biomedical Materials* 2010; **5(4)**, 44105.

[17] R Zhu, X Li, C Wu, L Du, X Du and T Tafsirojjaman. Effect of hydrothermal environment on mechanical properties and electrical response behavior of continuous Carbon Fiber/Epoxy composite plates. *Polymers* 2022; **14(19)**, 4072.

[18] H Qin, C Zhu, Z An, Y Jiang, Y Zhao, J Wang, X Liu, B Hui, X Zhang and Y Wang. Silver nanoparticles promote osteogenic differentiation of human urine-derived stem cells at noncytotoxic concentrations. *International Journal of Nanomedicine* 2014; **4**, 2469-2478.

[19] L Sethuram, J Thomas, A Mukherjee and N Chandrasekaran. Effects and formulation of silver nanoscaffolds on cytotoxicity dependent ion release kinetics towards enhanced excision wound healing patterns in Wistar albino rats. *RSC Advances* 2019; **9(61)**, 35677-35694.

[20] A Sati, TN Ranade, SN Mali, HKA Yasin and A Pratap. Silver nanoparticles (AgNPs): Comprehensive insights into bio/synthesis, key influencing factors, multifaceted applications, and toxicity - a 2024 update. *ACS Omega* 2025; **10(8)**, 7549-7582.

[21] S Maruelli, R Besio, J Rousseau, N Garibaldi, J Amiaud, B Brulin, P Layrolle, V Escriou and A Forlino. Osteoblasts mineralization and collagen matrix are conserved upon specific Col1a2 silencing. *Matrix Biology Plus* 2020; **6**, 100028.

[22] MG Kontakis, E Carlsson, C Palo-Nieto and NP Hailer. Ionic silver coating of orthopedic implants may impair osteogenic differentiation and mineralization. *Experimental and Therapeutic Medicine* 2025; **29(3)**, 51.

[23] Y Xu, B Zheng, J He, Z Cui and Y Liu. Silver nanoparticles promote osteogenic differentiation of human periodontal ligament fibroblasts by regulating the RhoA-TAZ axis. *Cell Biology International* 2019; **43(8)**, 910-920.

[24] E Dube and GE Okuthe. Silver nanoparticle-based antimicrobial coatings: Sustainable strategies for microbial contamination control. *Microbiology Research* 2025; **16(6)**, 110.

[25] T Liu, G Yang, T Li, Q Wang, H Liu and F He. Preparation of Ag@ 3D-TiO_2 scaffolds and determination of its antimicrobial properties and osteogenesis-p romoting ability. *Orthopaedic Surgery* 2024; **16(6)**, 1445-1460.

[26] SK Nemani, RK Annavarapu, B Mohammadian, A Raiyan, J Heil, A Haque, A Abdelaal and H Sojoudi. Surface modification of polymers: Methods and applications. *Advanced Materials Interfaces* 2018; **5(24)**, 1801247.

[27] R Subramani, RR Leon, R Nageswaren, MA Rusho and KV Shankar. Tribological performance enhancement in FDM and SLA additive manufacturing: Materials, mechanisms, surface

engineering, and hybrid strategies - a holistic review. *Lubricants* 2025; **13(7)**, 298.

[28] AG Khina and YA Krutyakov. Similarities and differences in the mechanism of antibacterial action of silver ions and nanoparticles. *Applied Biochemistry and Microbiology* 2021; **57(6)**, 683-693.

[29] A Merlo, E González-Martínez, K Saad, M Gomez, M Grewal, J Deering, LA DiCecco, Z Hosseinidoust, KN Sask, JM Moran-Mirabal and K Grandfield. Functionalization of 3d printed scaffolds using polydopamine and silver nanoparticles for bone-interfacing applications. *ACS Applied Bio Materials* 2023; **6(3)**, 1161-1172.

[30] NK Dhiman, S Agnihotri and R Shukla. Silver-based polymeric nanocomposites as antimicrobial coatings for biomedical applications. *In*: S Singh and P Maurya (Eds.). Nanotechnology in modern animal biotechnology: Recent trends and future perspectives. Springer, Singapore, 2019, p. 115-171.

[31] H Shao, T Zhang, Y Gong and Y He. Silver-containing biomaterials for biomedical hard tissue implants. *Advanced Healthcare Materials* 2023; **12(26)**, 2300932.

[32] M Harun-Ur-Rashid, T Foyez, SBN Krishna, S Poda and AB Imran. Recent advances of silver nanoparticle-based polymer nanocomposites for biomedical applications. *RSC Advances* 2025; **15(11)**, 8480-8505.

[33] Y Huang, Y Zhang, J Sheng, Z Li, W Zhang, J Shen, S Yang, J Zhong, L Yu and X Chen. Study on the preparation and properties of 3D-printed PETG/AgNPs antibacterial coatings for clear aligners. *Polymer Composites* 2025; **46(17)**, 15849-15860.

[34] C Yan, C Kleiner, A Tabigue, V Shah, G Sacks, D Shah and V DeStefano. PETG: Applications in modern medicine. *Engineered Regeneration* 2024; **5(1)**, 45-55.

[35] ME Astaneh and N Fereydouni. Silver nanoparticles in 3D printing: A new frontier in wound healing. *ACS Omega* 2024; **9(40)**, 41107-41129.

[36] MUA Khan, SIA Razak, H Mehboob, MRA Kadir, TJS Anand, F Inam, SA Shah, MEF Abdel-Haliem and R Amin. Synthesis and characterization of silver-coated polymeric scaffolds for bone tissue engineering: antibacterial and *in vitro* evaluation of cytotoxicity and biocompatibility. *ACS Omega* 2021; **6(6)**, 4335-4346.

[37] H Mishbak, MH Hassan, E Daskalakis, AM Omar, DM Freitas, W Mirihanage, P Mativenga, P Potluri and P Bartolo. Accelerated degradation of 3D-printed PETG bone-tissue scaffolds via geometrical control. *CIRP Annals* 2025; **74(1)**, 327-331.

[38] P Thadasri. 2020, Layer-by-layer surface modification of polymer filament for catalytic 3D printed parts. Master Thesis. Chulalongkorn University, Bangkok, Thailand.

[39] A Bharatish, A Kumar, KS Siddhanth, V Manikant, P Jagdish, A Sharma and S Solaiachari. On optimising wettability, surface roughness and swelling behaviour of laser-polished 3D-printed PETG polymer for bio-medical implants. *Polymer* 2025; **330**, 128482.

[40] AAA Al-Ali, KAS Alsalami and AM Athbi. Cytotoxic effects of CeO_2 NPs and β-Carotene and their ability to induce apoptosis in human breast normal and cancer cell lines. *Iraqi Journal of Science* 2022; **63(3)**, 923-937.

[41] M Marrese, V Guarino and L Ambrosio. Atomic force microscopy: A powerful tool to address scaffold design in tissue engineering. *Journal of Functional Biomaterials* 2017; **8(1)**, 7.

[42] J Iturri and JL Toca-Herrera. Characterization of cell scaffolds by atomic force microscopy. *Polymers* 2017; **9(8)**, 383.

[43] MUA Khan, SIA Razak, H Mehboob, MRA Kadir, TJS Anand, F Inam, SA Shah, MEF Abdel-Haliem and R Amin. Synthesis and characterization of silver-coated polymeric scaffolds for bone tissue engineering: Antibacterial and *in vitro* evaluation of cytotoxicity and biocompatibility. *ACS Omega* 2021; **6(6)**, 4335-4346.

[44] O Vasilev, A Hayles, D Campbell, R Jaarsma, L Johnson and K Vasilev. Nanoscale antibacterial coatings incorporating silver nanoparticles derived by plasma techniques - a state-of-the-art

perspective. *Materials Today Chemistry* 2024; **41**, 102341.

[45] M Shevtsov, E Pitkin, SE Combs, N Yudintceva, D Nazarov, GVD Meulen, C Preucil, M Akkaoui and M Pitkin. Biocompatibility analysis of the silver-coated microporous titanium implants manufactured with 3D-printing technology. *Nanomaterials* 2024; **14(23)**, 1876.

[46] NJ Shah, J Hong, MN Hyder and PT Hammond. Osteophilic multilayer coatings for accelerated bone tissue growth. *Advanced Materials* 2012; **24(11)**, 1445-1450.

[47] MA Sahebalzamani, TS Hashemi, ZM Nejad, S Agarwal, HO McCarthy, TJ Levingstone and NJ Dunne. Deposition of multilayer coatings onto highly porous materials by layer-by-layer assembly for bone tissue engineering applications using cyclic mechanical deformation and perfusion. *Materials Advances* 2024; **5(6)**, 2316-2327.

[48] HI Chang and Y Wang. Cell responses to surface and architecture of tissue engineering scaffolds. *In*: D Eberli (Ed.). Regenerative medicine and tissue engineering-cells and biomaterials. InTechOpen, London, 2011.

[49] F Afhkami, P Ahmadi and G Rostami. Cytotoxicity of different concentrations of silver nanoparticles and calcium hydroxide for MC3T3-E1 preosteoblast cell line. *Clinical and Experimental Dental Research* 2025; **11(1)**, e70075.